A reliable and efficient adaptive Bayesian method to assess static lower limb proprioception

Jonathan M Wood[1,2], *Susanne M Morton[1,2], *Hyosub E Kim[1,2,3]

*Both authors contributed equally

1. Department of Physical Therapy, University of Delaware, Newark, DE 19711, United States
2. Biomechanics and Movement Sciences Program, University of Delaware, Newark, DE 19711, United States
3. Department of Psychological and Brain Sciences, University of Delaware, Newark, DE 19716, United States

Abstract

Background

Lower limb proprioception is critical for maintaining stability during gait and may impact how individuals modify their movements in response to changes in the environment and body state, a process termed “sensorimotor adaptation”. However, the connection between lower limb proprioception and sensorimotor adaptation during human gait has not been established. We suspect this gap is due in part to the lack of reliable, efficient methods to assess global lower limb proprioception in an ecologically valid context.

New Method

We assessed static lower limb proprioception using an alternative forced choice task, administered twice to determine test-retest reliability. Participants stood on a dual-belt treadmill which passively moved one limb to stimulus locations selected by a Bayesian adaptive algorithm. At the stimulus locations, participants judged relative foot positions and the algorithm estimated the point of subjective equality (PSE) and the uncertainty of lower limb proprioception.

Results

Using the Bland-Altman method, combined with Bayesian statistics, we found that both the PSE and uncertainty estimates had good reliability.

Comparison with Existing Method(s)

Current methods assessing static lower limb proprioception do so within a single joint, in non-weight bearing positions, and rely heavily on memory. One exception assessed static lower limb proprioception in standing but did not measure reliability and contained confounds impacting participants’ judgments, which we experimentally controlled here.

Conclusions

This efficient and reliable method assessing lower limb proprioception will aid future mechanistic understanding of locomotor adaptation and serve as a useful tool for basic and clinical researchers studying balance and falls.

1. Introduction

Lower limb proprioception is critical for maintaining upright stability and regulating the gait cycle. The proprioceptive sense is formed through a combination of inputs, mostly from muscle spindles and Golgi tendon organs, but also cutaneous and joint capsule receptors (Proske and Gandevia, 2012). Here, we are most interested in proprioception as it relates to static lower limb position sense. Static lower limb position sense contributes to balance and stability as evidenced by studies showing that impaired static lower limb proprioception is associated with higher fall risk (Lord et al., 1991; Lord and Ward, 1994; Ribeiro and Oliveira, 2007). In addition to its contributions to posture and stability, static lower limb proprioception may also impact how individuals implicitly adapt their gait pattern in response to changes in the environment or body state (e.g., fatigue) (Bruijn et al., 2012; Bunday and Bronstein, 2009), a learning process termed "sensorimotor adaptation" (Prokop et al., 1995; Reisman et al., 2005). This link between static proprioception and sensorimotor adaptation is well established in upper-extremity reaching (Cressman and Henriques, 2009; Harris, 1963; Henriques and Cressman, 2012; Mattar et al., 2013; Ostry et al., 2010; Simani et al., 2007; Tsay et al., 2022). However, no causal link between proprioception and locomotor adaptation has been clearly established in humans, which is surprising given how dependent normal walking is on reliable proprioceptive estimates (Dietz, 2002; Hiebert et al., 1996; Kriellaars et al., 1994; Pearson, 2004; Roden-Reynolds et al., 2015; Whelan et al., 1995). We suggest that this discrepancy exists because of the way proprioception is measured in the lower limb. Specifically, most lower limb proprioception assessments are not performed in an ecologically valid context, and those that are lack established reliability and validity (Sombric et al., 2019; Vazquez et al., 2015). In order to address these limitations, we have developed a new psychophysical method for assessing lower limb proprioception.

We first considered the measurement of lower limb proprioception in a context that most closely approximates gait. Current methods assessing static lower limb proprioception often do so within a single joint, in a non-weight bearing position, and rely heavily on remembered positions (Han et al., 2016; Hillier et al., 2015; Horváth et al., 2022). While these methods have proven useful for characterizing specific deficits in joint proprioception after orthopedic injury (e.g., Relph et al., 2014), they cannot be readily translated to functional lower extremity movements. This is because a unified percept of limb location results from the nervous system's integration of proprioceptive signals across multiple limb joints (Bosco et al., 2000; Fuentes and Bastian, 2010; Gandevia, 1985; Proske and Gandevia, 2012; Soechting, 1982). The body position in which proprioception is measured is also important because differences in proprioceptive estimates emerge in weight bearing vs non-weight bearing positions both in the upper limb (Ansems et al., 2006) and in the knee joint (Bullock-Saxton et al., 2001; Stillman and McMeeken, 2001). For these reasons, we measured whole lower limb proprioception while standing as this provides the closest approximation to gait.

A comprehensive way of characterizing a sensory system is using a psychophysical assessment to estimate two of its distinct physiologic characteristics: the point of subjective equality (PSE) and the uncertainty. The PSE is the stimulus that is perceived as equal to another stimulus, reflecting the limits of a sensory system to discriminate between two stimuli. In the context of the current study, the PSE is the location where participants perceive the two lower limbs are symmetrical. The PSE can also be translated to a measure of proprioceptive accuracy by calculating the difference between the PSE and actual equality (i.e., a proprioceptive bias). Uncertainty refers to the variability in responses surrounding the PSE, reflecting the noise within the sensory system. The PSE (in terms of a proprioceptive bias) and uncertainty seem to play distinct roles in sensorimotor adaptation (Ruttle et al., 2021; Tsay et al., 2021). While upper extremity proprioceptive biases shift as a result of sensorimotor adaptation, proprioceptive

uncertainty at baseline predicts the magnitude of sensorimotor adaptation. The proprioceptive shift and uncertainty estimates themselves are uncorrelated (Tsay et al., 2021). Thus, it is important to reliably estimate both the PSE and uncertainty.

A widely accepted method of estimating both the PSE and uncertainty is to use a two-alternative forced choice (2AFC) task, where, in the context of the current study, participants judge the relative positions of their feet when placed at various locations. The response data are then fit with a psychometric function, where the inflection point (i.e., the probability of a response being 0.5), represents the PSE and the slope of the function is inversely proportional to the uncertainty (Kingdom and Prins, 2016). We know of two studies that used an AFC task to estimate both PSE and uncertainty of lower limb proprioception (Vazquez et al., 2015; Waddington and Adams, 1999). However, the Waddington study used active repositioning focused on only ankle inversion and eversion movements, whereas the Vazquez study did not measure or report the reliability of their method. Furthermore, in the latter study participants' responses were heavily impacted by the direction in which the test limb was moved to the stimulus position, which was either always forward or always backward depending on group assignment. Ideally, in a static assessment of lower limb proprioception, the movement of the limbs to stimulus positions should not exert any influence on participants' judgments. Therefore, while a method like the one used in the study by Vazquez and colleagues offers promise, adjustments are needed to improve the validity of responses, and the reliability of the estimates must be assessed.

Efficiency is also critical for assessing changes in proprioception in single-session motor learning studies, when considering factors such as clinical feasibility, and to maintain participant safety, as standing still for long periods can lead to syncope (Jardine et al., 2018). In the most established psychophysical method, the method of constant stimuli, participants make the same number of sensory judgements at each pre-determined stimulus location. However, this method is inefficient because some of the stimulus locations provide little information about the PSE or uncertainty estimates (Kingdom and Prins, 2016; Leek, 2001; Watson and Fitzhugh, 1990). Indeed, Kingdom and Prins (Kingdom and Prins, 2016, p. 57) suggested that as many as 400 trials are required to accurately estimate both the PSE and uncertainty. Adaptive psychophysical methods, where the stimulus locations are selected based on prior responses, were specifically developed to solve this efficiency problem (Leek, 2001). The Psi algorithm is one such method that uses Bayesian estimation to calculate PSE and uncertainty values after each trial. It then chooses the next stimulus that will maximize the information gained for both estimates on the subsequent trial (Kontsevich and Tyler, 1999). This method results in more efficient and accurate estimates of both the PSE and slope compared to the method of constant stimuli (King-smith and Rose, 1997; Kontsevich and Tyler, 1999; Livesey and Livesey, 2016; Turpin et al., 2010). The Psi algorithm is most frequently used in visual and auditory psychophysics, and we note only one instance where is was used to estimate (wrist) proprioception (Elangovan et al., 2018).

Here, we implemented an adapted version of the Psi algorithm and measured its reliability in assessing lower limb proprioception in an ecologically valid context using a test-retest design. We first wanted to ensure that participant responses were not confounded by the direction of movement to each stimulus location, a concern we had based on a prior study (Vazquez et al., 2015). Then, to assess reliability across test sessions, we calculated agreement, defined as the ability for a test to reproduce the same values when measured at different times, using the Bland-Altman method (Altman and Bland, 1983; Giavarina, 2015). In addition, we used Bayesian statistics to fully quantify the probability that the method has good agreement, defined as low evidence of bias in the PSE and uncertainty estimates across the two tests. Combined, we found that, with the current method, movement direction did not impact participant responses, and good agreement for both the PSE and uncertainty could be achieved after only 50 trials.

2. Materials and methods

2.1. Participants

Young healthy participants between the ages of 18 and 35 were recruited from the University of Delaware community. Participants were excluded if they had any chronic or recent musculoskeletal or neurologic diagnoses, pain, or impaired sensation. This work was completed in accordance with the Code of Ethics of the World Medical Association. All participants provided written informed consent prior to being enrolled into the study. This study was approved by the University of Delaware Institutional Review Board.

2.2. Motion capture

Participants stood on a dual-belt treadmill instrumented with two force plates, one under each belt (Bertec, Columbus OH). We obtained kinematic data, sampled at 100Hz, using an eight-camera Vicon MX40 motion capture system with Nexus software (Vicon Motion Systems Inc., London, UK). Seven retroreflective markers were placed on participants' shoes and ankles in the following locations: bilateral heels, bilateral lateral malleoli, bilateral 5th metatarsal head, and the left 1st metatarsal head. We used custom written MATLAB scripts (version 2022a, MathWorks, Natick, MA) to control the treadmill belts and obtain live kinematic and kinetic data from Nexus software.

2.3. AFC task

We used a two-AFC task to measure lower limb proprioception. To measure test-retest reliability, each participant performed the test twice on the same day, with a 20-minute break between tests. For each test, participants stood on a treadmill with vision of their legs occluded with a black drape, and auditory feedback (sounds of the treadmill belts/motors) occluded with noise cancelling headphones (Figure 1A). The primary kinematic variable for the test was foot position difference (in millimeters):

$$Foot\ position\ difference = Left\ marker_{Ypos} - Right\ marker_{Ypos} \quad (1)$$

We used the lateral malleoli markers to measure foot position difference. Thus, positive values indicate the left foot was forward of the right foot, while negative values indicate the left foot was behind. Since the foot is the end-effector for the lower limb, we assume judgements were made by combining proprioceptive information across lower limb joints. The right foot served as the reference foot and did not move throughout the test. The left foot served as the test foot and was passively moved by the left treadmill belt to the stimulus positions, measured in terms of foot position difference. After participants performed two practice trials to orient them to the task, their heels were aligned so that everyone started from the same position relative to the laboratory's y-axis. Since there may still be differences in the ankle markers along the y-axis in this position, we corrected for this baseline difference (rounded to the nearest millimeter) for stimulus positions and PSE estimates. Each test was comprised of 75 trials, and each trial had two parts: 1) movement to a start position, 2) movement to a stimulus position.

The treadmill moved the test foot to a start position at a speed selected from a uniform distribution between 40 and 50 mm/s (Figure 1B, top). We controlled for the potential bias in responses caused by movement direction by providing pseudorandomized start positions so that the test foot started in front of the stimulus position 38 times and behind the stimulus 37 times. Therefore, we assume any bias in responses from always moving to the stimulus from the same direction

would be washed out, something we confirmed in our formal analysis (see Section 3.1). The specific start position on a given trial, t, was selected from one of two normal distributions centered around either -100 or +100 mm of foot position difference depending on the movement direction for that trial. Both distributions had a standard deviation of 5 mm:

$$Start\ position_{[t]} \sim \begin{cases} \mathcal{N}(+100, 5), & if\ movement\ direction_{[t]} == backward \\ \mathcal{N}(-100, 5), & if\ movement\ direction_{[t]} == forward \end{cases} \quad (2)$$

After a 0-2 second pause at the start position, the test foot was moved to a stimulus position at a speed selected from a uniform distribution between 10 and 30 mm/s (Figure 1B, bottom). The stimulus positions were located at 21 possible foot difference locations: every 10 mm interval between -100 to +100 mm. Most stimulus positions were selected using the Psi algorithm (see section 2.5). However, we inserted pre-selected stimulus locations to keep participants engaged in the task. There were two types of pre-selected stimuli: 1) far stimuli (±100 or ±90) inserted randomly once every 10 trials, and 2) near stimuli (±10, ±20 or ±30 mm from the current PSE estimate, rounded to the nearest stimulus location) inserted randomly once every 5 trials. No preselected stimuli were inserted within the first 5 trials.

Each time the test foot reached its stimulus position, the treadmill stopped, and a prompt appeared on a monitor in front of the participant: “Do you feel your right or left foot is more forward?” The participant’s response was recorded by the experimenter using a custom graphical user interface (GUI) in MATLAB.

Before the test, participants were instructed to keep their weight equally distributed between both feet, measured with the force plates under each treadmill belt and displayed for the experimenter. If participants consistently kept greater than ~60% of their weight through one foot, a verbal reminder was provided. We implemented short breaks after 25 and 50 trials to prevent fatigue and blood pooling in the legs. Before the break, current marker positions were recorded from Nexus software, then the participant was asked to walk around the lab for ~30 seconds. After the participant stepped back onto the treadmill, we positioned their feet so the ankle markers were back to the exact location from which they started and then testing continued.

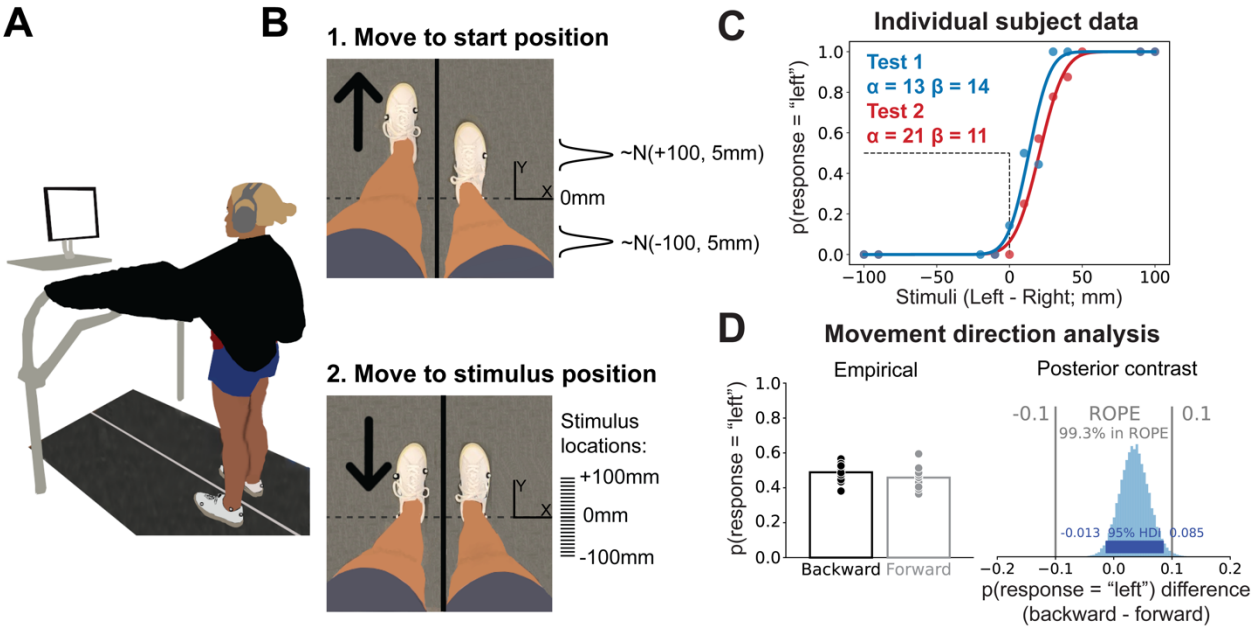

Figure 1. Task setup, representative data, and movement direction analysis. (A) AFC task setup. Participants stood on the split-belt treadmill with visual feedback of their legs occluded by a black drape and auditory feedback occluded by noise cancelling headphones. The screen prompted participants to verbally respond to the question "Do you feel like your right or left foot is more forward?" when the test foot stopped at the stimulus location. **(B)** Trial sequence. 1) The test foot was moved to a start position either in front of or behind the stimulus position. Start positions were sampled from one of two normal distributions, depending on the movement direction assigned for that specific trial. 2) The test foot was moved to one of 21 possible stimulus positions between -100 and +100 mm. Tick marks (drawn to scale) represent each possible stimulus location. **(C)** Individual participant data. We reconstructed the psychometric functions from the PSE (α) and uncertainty (β) estimates for Test 1 (blue) and Test 2 (red). The dashed black lines, provided as a reference, represent a PSE of 0 mm. The individual dots represent the participant's response data for each test. **(D)** Movement direction analysis. We measured the mean empirical probability of responding left when the movement direction to the stimulus position was forward (gray) vs backward (black). Dots represent individuals. We also used a Bayesian logistic regression model to analyze the unique impact of each movement direction on participant responses by calculating the difference between the posterior estimates of the movement direction coefficients (one for forward movement, one for backwards) of every participant, yielding a posterior contrast distribution (histogram) which we compared to a region of practical equivalence (ROPE). We note that 99.3% of the posterior distribution is within the ROPE, confirming that responses were not biased by movement direction to the stimulus position.

2.4. Psychometric function

Each participant's probability of responding that the test foot was more forward at each stimulus position (x) was represented as a normal cumulative distribution function (cdf) with two parameters:

$$\psi(x) = normcdf(x; \alpha, \beta) \tag{3}$$

The α parameter, the mean or inflection point of the cdf, represents the PSE, corresponding to the position that the participant perceives the feet were in the same location along the laboratory's y-axis (i.e., where the probability of judging "left" is exactly 0.5). The β parameter, the standard deviation of the cdf, represents the uncertainty, which reflects the noise within the sensory system itself. Both are measured in terms of foot position difference. The α and β parameters were estimated adaptively on each trial using the Psi algorithm. Of note, in our pilot testing the probability of responding left at -100 and +100 was consistently 0 or 1, respectively. Thus, we did not include the lapse and guess rate parameters that are sometimes used in psychometric functions for AFC tasks.

2.5. Psi Algorithm

Here we provide a brief description of the Psi algorithm, which is described in detail by Kostovich and Tyler (1999). There are two primary components of the Psi algorithm: 1) stimulus selection and 2) parameter estimation.

2.5.1 Stimulus selection

Before each trial, the Psi algorithm simulates responses at each possible stimulus location for the next trial, calculating a simulated joint posterior distribution using Bayes' rule. The simulated joint posterior distribution (p_{sim}) contains the probability of every possible combination of α and β values given the simulated responses and the stimulus location. Information entropy (H), a measure of the magnitude of uncertainty in a probability distribution, is calculated for each stimulated posterior distribution:

$$H_{[x]} = -\sum_{i} p_{sim[i]} log_2 p_{sim[i]} \tag{4}$$

The stimulus position that minimizes the information entropy is selected for the subsequent trial as it provides the most certainty and thus the greatest gain in information for the α and β estimates from the current trial to the next (Shannon, 1948). That is, the stimulus position that will theoretically aid in maximally efficient parameter estimation is selected on each trial.

2.5.2 Parameter estimation

Once the participant makes their selection at the stimulus location, the Psi algorithm uses Bayes' rule to estimate the most likely α and β values given the prior and the current response (r):

$$p_{[t]}(\lambda|x,r) = \frac{p_{[t]}(\lambda)p(r|\lambda,x)}{\sum_{\lambda}\left(p_{[t]}(\lambda)p(r|\lambda,x)\right)} \quad (5)$$

The prior, $p_{[t]}(\lambda)$, is a joint probability distribution representing the initial guess of α and β values. The prior for the first trial was the same for all participants. We assumed that the most likely α was 0 with a wide standard deviation: $\alpha \sim N(0,20)$. Similarly, we assumed a reasonably wide prior distribution for β, with an expected value of 20: $\beta \sim Exponential(20)$. On subsequent trials, the posterior for trial t became the prior for trial t+1 ($p_{[t+1]}(\lambda) = p_{[t]}(\lambda|x,r)$). The likelihood in equation 5, $p(r|\lambda,x)$, is the probability of the participant's response given each parameter value at the stimulus position. As suggested by Kostovich and Tyler, we created a pair of lookup tables to improve computational efficiency, one for each response, which served as indexable likelihoods for each stimulus:

$$p(r = \text{"}left\text{"}|\lambda,x) = \psi \quad (6a)$$
$$p(r = \text{"}right\text{"}|\lambda,x) = 1 - \psi \quad (6b)$$

The individual α and β estimates were calculated by marginalizing over the joint posterior distribution (equation 5) and taking the mean of each marginalized distribution (Emerson, 1986). We used the final α and β estimates after the last (75th) trial for our agreement analyses.

2.7. Statistical analysis

We used a Bayesian approach to make statistical inferences for the validity of responses and the agreement of PSE and uncertainty estimates. This approach enabled us to calculate the full posterior probability distribution of model parameters, providing a complete picture that quantifies our uncertainty. Thus, it naturally emphasizes estimation over binary decision rules in accordance with recommendations made by the American Statistical Association and others (Kruschke, 2013; Kruschke and Liddell, 2018; Wasserstein and Lazar, 2016).

For each analysis, we started by defining a statistical model that was consistent with our question and the data structure. Next, we calculated the posterior probability of all parameter values in the statistical model using Bayes' rule, combining our prior assumptions regarding parameter values (i.e., the prior) with evidence from our data (i.e., the likelihood). We selected the distribution for each parameter's prior as reasonably wide and uninformative, using its maximum entropy distribution (McElreath, 2016). We used the Pymc4 (version 4.3) library (Salvatier et al., 2016) in Python (version 3.11) to perform Markov Chain Monte Carlo (MCMC) sampling to estimate the posterior probability distributions. We drew 10,000 samples from the posterior in each of 4 chains (i.e., 40,000 total samples), using 2,000 tuning samples in each chain. We performed diagnostics for each model, ensuring parameter values were consistent across chains and checking posterior

estimates for possible errors (Kruschke, 2014; McElreath, 2016). We provide the full models and code, including detailed information about the priors and diagnostics, online at (https://osf.io/g8nx4/). We made inferences based on the posterior distribution of the model parameters, reporting the 95% high density interval (HDI), defined as the narrowest span of credible values that contains 95% of the posterior distribution (Kruschke, 2014). In cases in which we wanted to quantify support for the "null" hypothesis, we also calculated the percent of credible parameter values that fell within a region of practical equivalence (ROPE; Kruschke, 2014).

First, we ensured that responses were not confounded by movement direction, a concern based on a prior study (Vazquez et al., 2015). We modeled each participant's response data using a Bayesian logistic regression. Since the response data on each trial (t) were binary, we modeled them as a Bernoulli distribution where the probability of responding "left" (p_{left}) was impacted by the stimulus location ($X_{Stimulus}$), the movement direction ($\beta_{Move\ direction}$), and the participant ($\alpha_{Participant}$):

$$Response_{[t]} \sim Bernoulli\left(p_{left[t]}\right) \quad (7a)$$

$$logit\left(p_{left[t]}\right) = \alpha_{Participant[i]} + \beta_{Movedirection[j]} + \beta_{Stimulus} X_{Stimulus[t]} \quad (7b)$$

We included data from both tests for each participant in this model. Stimulus position was coded as a continuous variable. Movement direction and participant were coded as indexing variables, meaning separate $\alpha_{Participant}$ posteriors were computed for each participant (i; 13 total alphas), representing each participant's bias to judge "left" independent of movement direction or stimulus position, and two separate group level $\beta_{Move\ direction}$ posteriors were computed for each movement direction (j; forward and backward; 2 total $\beta_{Move\ direction}$ parameters) to the stimulus position. We reasoned that if moving forward or backward had no influence on responses, the two posterior distributions for $\beta_{Move\ direction}$ should be identical. We therefore calculated the difference in probability between the $\beta_{Move\ direction}$ posterior distributions, setting a ROPE for this contrast between -0.1 and 0.1 in terms of probability.

To assess test-retest agreement, we used the Bland-Altman method (Altman and Bland, 1983; Giavarina, 2015). The Bland-Altman method is recommended to assess agreement because it specifically tests for biases across the range of "true" scores of a given variable, where a proxy for the true score is the mean of an individual's score on Test 1 and Test 2 (Bland and Altman, 1986). The method involves 3 analyses: 1) calculating the mean bias between the two estimates, 2) calculating the bias across "true" values, and 3) determining the limits of agreement, calculated as the mean of the difference in estimates ±1.96 times the standard deviation of the difference in estimate. To test for biases in steps 1 and 2 we applied Bayesian inference instead of the frequentist methods typically used in the Bland-Altman method. We determined if there was a mean bias by estimating the distribution of differences between Test 1 and Test 2 for the PSE and uncertainty estimates separately. We modeled these contrasts as a normal distribution, estimating the most likely μ and σ values that could have generated each individual's (i) estimated difference from Test 1 to Test 2:

$$Difference_{[i]} \sim Normal(\mu, \sigma) \quad (8)$$

We focused our inference on the posterior distribution for μ, which, if no bias was present, should be close to zero. We therefore set a ROPE between -5 and 5 mm. We determined if there was a bias across the range of "true" values of PSE and uncertainty using a Bayesian regression analysis. The outcome variable, differences between Test 1 and Test 2 estimates for each

participant ($Y_{[i]}$), was modeled as a normal distribution with the mean (μ) being predicted by the "true" PSE/uncertainty value (X_{true}):

$$Y_{[i]} \sim Normal(\mu_{[i]}, \sigma) \quad (9a)$$

$$\mu_{[i]} = b + m\, X_{true[i]} \quad (9b)$$

Here, a bias will manifest as an intercept (b) and slope (m) with magnitudes greater than 0. Therefore, we set a ROPE for the intercept between -5 and 5 mm and a ROPE for the slope between -0.1 and 0.1, which would translate to a 1 mm change in bias for a 10 mm change in "true" score. We defined good agreement as little to no evidence of a mean bias or a bias across true scores. Specifically, 90% of the posterior distributions calculated in the Bland-Altman analysis should not fall outside the ROPEs. We also performed a secondary analysis to determine if perfect agreement was at least plausible by characterizing the relationship between Test 1 and Test 2 for both the PSE and uncertainty estimates. Perfect agreement would result in a slope of 1 and an intercept of 0. We again used a Bayesian regression model, except the estimate on Test 2 was the outcome variable ($Y_{Test\ 2}$) and the estimate on Test 1 was the predictor variable ($X_{Test\ 1}$):

$$Y_{Test\ 2[i]} \sim Normal(\mu_{[i]}, \sigma) \quad (10a)$$

$$\mu_{[i]} = b + m\, X_{Test\ 1[i]} \quad (10b)$$

Here the HDIs for m characterize the relationship between Test 1 and 2.

3. Results and discussion

3.1. Movement direction did not influence participant responses

Thirteen participants (8 female, 5 male) completed the study. Data for one representative participant are displayed in Figure 1C. The psychometric functions (solid curves) were produced from the PSE (α) and uncertainty (β) estimates after the 75th trial and superimposed onto the empirical data (dots). For both tests, PSE values were positively biased (Test 1 mean [95% HDI] = 12.0 mm [3.3 20.6]; Test 2 = 15.3 mm [5.3 25.2]) and uncertainty measures (i.e., SDs) were just under 20mm (Test 1 = 18.2 mm [14.4 21.8]; Test 2 = 17.5 mm [13.5 21.4]). Our first concern, based on a prior study (Vazquez et al., 2015), was to ensure that we controlled for the potential confound that movement direction may have had on responses. While the empirical probability of responding left when moving backward and forward (Figure 1D, left) appear similar, we also determined the individual impact of movement direction on responses using a Bayesian logistic regression. If movement direction did play a major role in responses, the difference in probabilities for $\beta_{Move\ direction\ [Forward]}$ vs $\beta_{Move\ direction\ [Backward]}$ would be large, making the contrast largely different from 0. However, we found that the movement direction contrast was practically equal to 0 (Figure 1D, right; posterior mean [95% HDI], contrast = 0.04 [-0.01, 0.09], 99.3% in the ROPE). Thus, randomizing the start positions prevented biased responses.

3.2. Bland-Altman analysis revealed good agreement for both PSE and uncertainty estimates

We used the Bland-Altman method to assess agreement (Figure 2A). First, we calculated the limits of agreement for PSE and uncertainty estimates (-22.3 to 15.5 mm and -10.1 to 11.6 mm, respectively; dotted lines in Figure 2A). Limits of agreement for both were relatively narrow considering the scale of the measurement, and the PSE limits were consistent with the range of values observed in previous work (Vazquez et al., 2015) which used 33 more trials than the current method. Next, we characterized the mean bias between Test 1 and Test 2 for PSE and

uncertainty estimates (histograms in Figure 2A). Both biases were very close to 0. The average bias for PSE was -3.3mm [-9.0, 2.8] (72.4% in ROPE). In other words, while the PSE was nominally lower on Test 2 than Test 1, we can be fairly confident that there is little-to-no bias for PSE measurements. With regard to uncertainty estimates, there was effectively no bias as the 95% HDI was fully within the ROPE (0.7mm [-2.8, 4.1], 98.8% in ROPE).

Next, we tested for evidence of a bias across different "true" PSE and uncertainty estimates, where the true estimate is represented by the mean of an individual's estimates on Test 1 and Test 2 (i.e., the x-axis in the Bland-Altman plot), using a Bayesian linear regression model (solid regression line and shading in Figure 2A). For PSE, there was a small negative slope, although the most credible estimates surrounded a slope estimate of zero (-0.15 [-0.56, 0.28], 29.6% in ROPE), and the intercept was unbiased (-1.3 [-9.5 6.9], 76.0% in ROPE). These results indicate that participants with larger PSE values tend have increased bias between test 1 and 2. However, even when considering the largest mean PSE of ~40mm, this only produces a bias of -6mm. Therefore, we interpret this bias as negligible. For uncertainty estimates, the most probable regression was very similar to a line with 0 slope and 0 intercept (slope = -0.08 [-0.69, 0.58], 24.5% in ROPE; intercept = 2.0 [-9.8, 13.8], 58.4% in ROPE). Combined, both Bland-Altman results show that estimated PSE and uncertainty values remain largely consistent across test-retest sessions and across the range values, a sign of good agreement for this method.

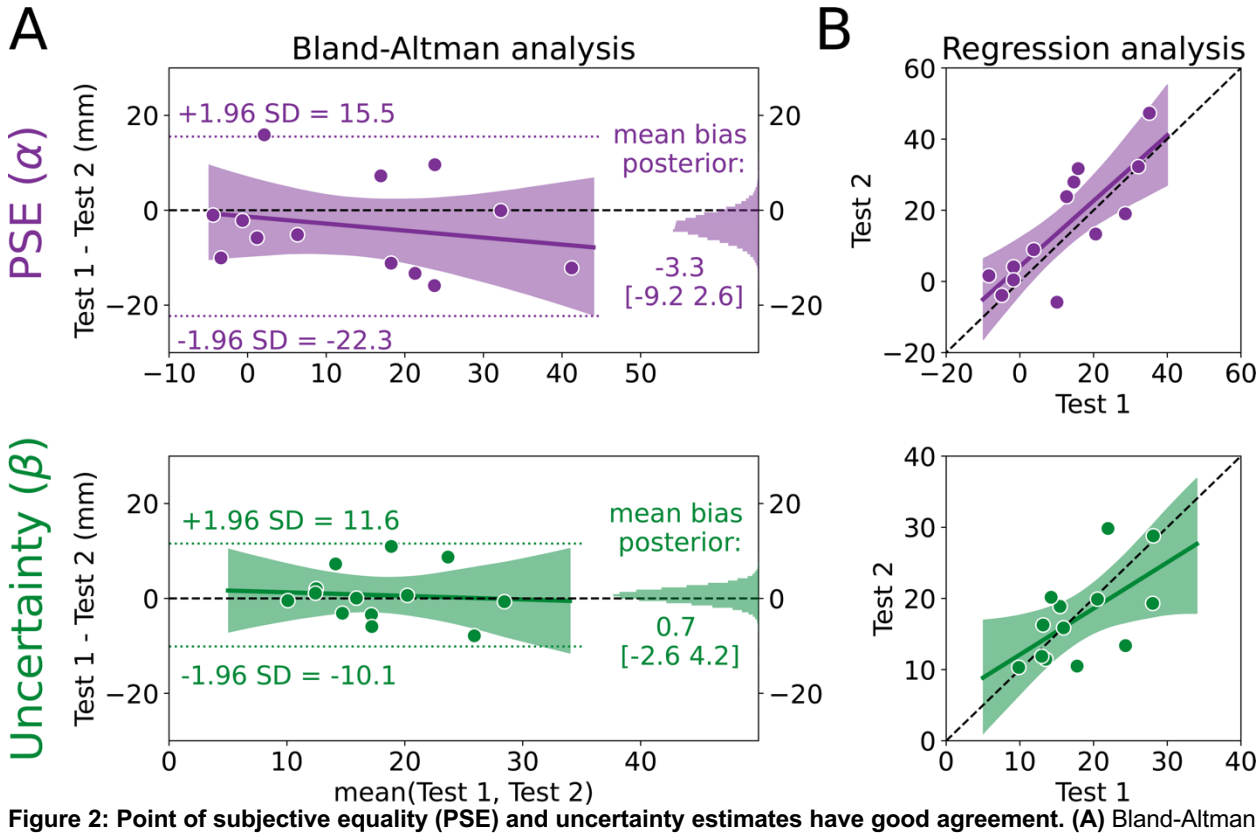

Figure 2: Point of subjective equality (PSE) and uncertainty estimates have good agreement. (A) Bland-Altman plot for the PSE (α; top) and uncertainty (β; bottom) estimates. The mean of Test 1 and Test 2 for each individual is plotted on the x-axis and the difference between the two tests is plotted on the y-axis. Thus, each dot represents one individual. The limits of agreement are plotted as the dotted lines, and the posterior distributions for the mean biases are plotted on the right sides as histograms. The most probable regression line is the solid line with the shading representing the 95% high density interval (HDI), with the black dashed line at 0 as a reference **(B)** Regression model for PSE and uncertainty. Estimates for Test 2 are plotted against estimates for Test 1 for each individual (dots) with the unity line (black dashed line) provided as a reference for perfect agreement. The most probable regression line is the solid line with the shading representing the 95% HDI.

As a secondary analysis, we characterized the relationship between estimates on Test 1 and Test 2 to determine if something close to perfect agreement (slope=1, intercept=0) was at least plausible, again using a Bayesian linear regression model. Whereas the Bland-Altman analysis uses information from the two tests to estimate a "true" score (the x-axes in Fig 2A), the regression analysis measures the difference between the two tests without sharing information across tests. Figure 2B shows the most credible regression lines for PSE (top) and uncertainty (bottom) estimates, with the shading representing the 95% HDI. While there were credible slope values that fell both above and below one (slope = 0.92 [0.49, 1.38], intercept = 4.2 [-3.7, 12.4]), the single best PSE estimate (maximum a posteriori) between Tests 1 and 2 was very nearly one. The uncertainty estimates indicated that this parameter is less likely to perfectly reproduce the scores on Test 1 and Test 2 (slope = 0.65 [0.09, 1.19], intercept = 5.6 [-5.1, 15.8]). Interestingly, the results of this secondary analysis seemingly conflict with the Bland-Altman analysis. However, we see them as complementary: While the average bias is low and consistent across scores, the uncertainty values are less likely to be exactly reproduced from Test 1 to Test 2 compared to the PSE values. This might be interpreted as a reduction in uncertainty from Test 1 to Test 2 indicating a practice effect, however, individuals with lower uncertainty on Test 1 demonstrated increased uncertainty on Test 2. Consistent with reports in other psychophysical assessments, measures of uncertainty are more difficult to recover compared to PSE (King-smith and Rose, 1997; Kontsevich and Tyler, 1999; Turpin et al., 2010). Together, the results of this secondary analysis suggest that, while there is evidence of variability across test sessions, it is well within an acceptable range for psychophysical assessment. Indeed, the 95% HDI for PSE and uncertainty estimates both included what we would expect if the tests had perfect agreement.

As further evidence of good agreement in our method, and to make direct comparisons with other studies, we also calculated intraclass correlation coefficients ($ICC_{2,1}$), another commonly used metric of agreement (Berchtold, 2016; Kottner et al., 2011; McGraw and Wong, 1996). The ICC values for PSE ($ICC_{2,1}$ [95% CI] = 0.80 [0.48, 0.93]) and uncertainty (0.61 [0.05, 0.85]) indicate good agreement (Portney and Watkins, 2009). These values fall within ranges of other psychophysics studies using the Psi algorithm and the method of constants, as those studies report ICCs for PSE estimates that range between 0.48 to 0.96 for the Psi algorithm (Schilling et al., 2017; Silva et al., 2020), and between 0.77 to 0.88 for the method of constants (Nicholson et al., 1997). Our method also compares favorably to other proprioception-specific assessments with ICCs ranging from 0.11 to 0.95 for measures of proprioceptive accuracy (Antcliff et al., 2021; Arvin et al., 2015; Deshpande et al., 2003; Gorst et al., 2020; Hillier et al., 2015; Rinderknecht et al., 2018), and from 0.0 to 0.64 for measures of proprioceptive variability (Juul-Kristensen et al., 2008; Rahlf et al., 2019; Strong et al., 2021). The fact that the current method has good agreement for both proprioceptive PSE and uncertainty opens the door for future studies to assess the importance of uncertainty to lower limb function.

3.3. Agreement was similar after 50 trials

One of our primary goals for this method was to maximize efficiency. Participants took an average of 20±1 minutes to complete testing (including the two short walking breaks). The simplest way to reduce this time would be to reduce the number of trials, however, there is a risk that reducing the number of trials would also reduce the agreement of the PSE and uncertainty estimates. Since the Psi algorithm estimates PSE and uncertainty after every trial, we can assess agreement after any trial during the test. As a post-hoc analysis, we chose to assess agreement after 50 trials as the test time at this point would have been between 10-15 minutes. We found that all our measures of agreement were similar after 50 and 75 trials (Table 1). In contrast, examining agreement after 25 trials revealed a substantial reduction in agreement. Therefore, decreasing the number of trials to 50 would significantly reduce the time of the test without sacrificing

agreement, providing a reasonable timeframe for a test to be placed in the middle of a motor learning paradigm or to be used for a balance and falls risk assessment.

Table 1: Agreement comparison after 50 and 75 trials

	Limits of agreement (mm)	Bland Altman Mean Bias (mm; % in ROPE)	Bland Altman Bias Regression (mm; % in ROPE)	Test 1 vs Test 2 Regression	$ICC_{2,1}$ [95% CI]
PSE (α)					
50 trials	-22.3 to 15.7	-3.2 [-9.2 2.6] (73.5%)	Slope = -0.17 [-0.61 0.29] (26.2%) Intercept = -1.1 [-9.3 7.1] (77.0%)	Slope= 0.91 [0.45 1.40] Intercept = 4.1 [-3.9 12.0]	0.78 [0.43, 0.92]
75 trials	-22.3 to 15.5	-3.3 [-9.0 2.8] (72.4%)	Slope = -0.15 [-0.56 0.28] (29.6%) Intercept = -1.3 [-9.5 6.9] (76.0%)	Slope= 0.92 [0.49 1.38] Intercept = 4.2 [-3.7 12.4]	0.80 [0.48, 0.93]
Uncertainty (β)					
50 trials	-9.3 to 10.2	0.5 [-2.7 3.5] (99.5%)	Slope = 0.03 [-0.65 0.69] (24.3%) Intercept = 0.0 [-12.5 12.2] (60.0%)	Slope= 0.57 [0.03 1.09] Intercept = 7.4 [-2.8 17.4]	0.58 [0.05, 0.85]
75 trials	-10.1 to 11.6	0.7 [-2.8 4.1] (98.8%)	Slope = -0.08 [-0.69 0.58] (24.5%) Intercept = 2.0 [-9.8 13.8] (58.4%)	Slope= 0.65 [0.09 1.19] Intercept = 5.6 [-5.6 15.8]	0.61 [0.05, 0.86]

3.4. Limitations and future directions

Despite the efficiency and good agreement of this method, we also recognize some of its limitations. For instance, one way to increase ecological validity when measuring proprioception would be to assess three-dimensional position sense as opposed to measuring proprioception in only the sagittal plane as we have done here. However, we believe our results should at least generalize to locomotor adaptation on the split-belt, given that, in this context, adaptation is often measured in sagittal plane kinematics like step length (Reisman et al., 2005). Another potential limitation is that during standing, although participants' limbs were passively moved by the motorized treadmill, it is impossible to avoid some subtle movements and associated muscle activity. While no overt movements were observed during testing, in theory, any voluntary muscle activity might provide additional information about where the limb is located due to an efference copy of the motor command (Wolpert et al., 1995). However, in our case, such a compromise was unavoidable, as the primary goal of this study was to develop an assessment of lower limb position sense in a context that most closely resembles gait.

In addition to measuring proprioception in standing, we assessed position sense of the whole lower limb by asking individuals to focus on the end effector (foot position) when making their judgements. Interestingly, there are few static lower extremity proprioception studies that ask individuals to focus on end effector position (but see Sigmundsson et al., 2000; Vazquez et al., 2015), despite the functional significance of foot position to successful gait (e.g., stepping over curbs, trail running, etc.). Conversely, upper extremity studies frequently assess whole limb proprioception by having participants make judgments regarding end effector position (hand or finger (Jones et al., 2010; Vindras et al., 1998). These methods have characterized the precision of limb position sense (van Beers et al., 1998), the relationship between static proprioception and voluntary reaching movements (Jones et al., 2010), and the importance of static proprioception to sensorimotor adaptation (Clayton et al., 2014; Cressman and Henriques, 2010; Simani et al., 2007; Tsay et al., 2021; van Beers et al., 2002). Unfortunately, similar lines of research are absent in locomotion, despite the critical role of proprioception in walking (Hiebert et al., 1996; Kriellaars et al., 1994; Pearson, 2004; Roden-Reynolds et al., 2015; Whelan et al., 1995). We speculate this is due at least in part to the previous absence of reliable and efficient methods of assessing lower limb proprioception in an upright, functional, and multi-joint context. We hope the current method opens the door to increasing understanding of the relationship between lower limb proprioception and locomotor adaptation in young, neurotypical adults as well as in older and

neurologic populations, for whom changes in proprioception may have a significant impact on their ability to adapt gait patterns (Bruijn et al., 2012; Bunday and Bronstein, 2009; Lam and Pearson, 2002; Pearson, 2000; Santuz et al., 2022).

Efficient and reliable, whole lower limb proprioceptive measurements during standing should be useful for non-adaptation studies as well. For example, proprioception is an important part of multifactorial falls assessments (Lord et al., 1991), but the proprioception test previously recommended involves active toe position matching in a non-weight bearing position. The current method offers a more ecologically valid lower limb proprioception test since it is much closer in context to when falls most often occur: during weight bearing activities like walking and transfers (Talbot et al., 2005). Furthermore, since most lower limb proprioception tests only measure proprioceptive accuracy or bias (Han et al., 2016; Hillier et al., 2015; Horváth et al., 2022), it is unknown how proprioceptive uncertainty may relate to falls, something that can now be empirically assessed using the current method.

As there are very few studies reporting PSE and uncertainty values for the lower limbs, we were interested in comparing our values to those reported in upper extremity studies. We found that the average uncertainty estimates in the present study were quite similar to values found in upper extremity proprioception studies (Jones et al., 2010), with both falling just under 2 cm. Additionally, we found that PSE estimates here were biased, a finding consistent with intrinsic biases in perceived hand/arm position (Fuentes and Bastian, 2010; Ingram et al., 2019; Jones et al., 2010; van Beers et al., 1996). We note that the bias reported in the present study is not related to footedness, nor due to moving only the left limb, as we randomized the test limb during pilot testing and found no difference in PSE values when the left versus the right limbs were moved. Importantly, biased estimates in upper extremity studies have been linked to biases in reaching direction (Jones et al., 2010; Vindras et al., 1998), suggesting that future work in the lower extremities may benefit from examining whether PSE biases are related to step length or other gait-related movements.

4. Conclusion

We developed and tested the reliability of a lower limb proprioception assessment in a gait-specific context. This method is efficient, requiring only 50 trials to reliably estimate both the PSE and uncertainty of lower limb proprioception. We believe this method will aid future mechanistic understanding of locomotor adaptation and serve as a useful tool for basic and clinical researchers studying balance and falls.

Acknowledgements

This work was supported by the National Institutes of Health [K12- HD055931 (HEK), R01-AG071585 (SMM), S10-RR028114 (SMM)], the National Science Foundation [M3X 1934650 (HEK)], and partial funding from the University of Delaware Graduate College (JMW). We want to extend a special thank you to Saunders Penn for his help creating Figure 1A and B and for his help performing data collections.

References

Altman, D.G., Bland, J.M., 1983. Measurement in Medicine: The Analysis of Method Comparison Studies. J. R. Stat. Soc. Ser. Stat. 32, 307–317. https://doi.org/10.2307/2987937

Ansems, G.E., Allen, T.J., Proske, U., 2006. Position sense at the human forearm in the horizontal plane during loading and vibration of elbow muscles. J. Physiol. 576, 445–455. https://doi.org/10.1113/jphysiol.2006.115097

Antcliff, S., Welvaert, M., Witchalls, J., Wallwork, S.B., Waddington, G., 2021. Assessing Proprioception in an Older Population: Reliability of a Protocol Based on Active Movement Extent Discrimination. Percept. Mot. Skills 128, 2075–2096. https://doi.org/10.1177/00315125211029906

Arvin, M., Hoozemans, M.J.M., Burger, B.J., Verschueren, S.M.P., van Dieën, J.H., Pijnappels, M., 2015. Reproducibility of a knee and hip proprioception test in healthy older adults. Aging Clin. Exp. Res. 27, 171–177. https://doi.org/10.1007/s40520-014-0255-6

Berchtold, A., 2016. Test–retest: Agreement or reliability? Methodol. Innov. 9, 2059799116672875. https://doi.org/10.1177/2059799116672875

Bland, J.M., Altman, D.G., 1986. Statistical methods for assessing agreement between two methods of clinical measurement. Lancet Lond. Engl. 1, 307–310.

Bosco, G., Poppele, R.E., Eian, J., 2000. Reference Frames for Spinal Proprioception: Limb Endpoint Based or Joint-Level Based? J. Neurophysiol. 83, 2931–2945. https://doi.org/10.1152/jn.2000.83.5.2931

Bruijn, S.M., Van Impe, A., Duysens, J., Swinnen, S.P., 2012. Split-belt walking: adaptation differences between young and older adults. J. Neurophysiol. 108, 1149–1157. https://doi.org/10.1152/jn.00018.2012

Bullock-Saxton, J.E., Wong, W.J., Hogan, N., 2001. The influence of age on weight-bearing joint reposition sense of the knee. Exp. Brain Res. 136, 400–406. https://doi.org/10.1007/s002210000595

Bunday, K.L., Bronstein, A.M., 2009. Locomotor adaptation and aftereffects in patients with reduced somatosensory input due to peripheral neuropathy. J. Neurophysiol. 102, 3119–3128. https://doi.org/10.1152/jn.00304.2009

Clayton, H.A., Cressman, E.K., Henriques, D.Y.P., 2014. The effect of visuomotor adaptation on proprioceptive localization: the contributions of perceptual and motor changes. Exp. Brain Res. 232, 2073–2086. https://doi.org/10.1007/s00221-014-3896-y

Cressman, E.K., Henriques, D.Y.P., 2010. Reach Adaptation and Proprioceptive Recalibration Following Exposure to Misaligned Sensory Input. J. Neurophysiol. 103, 1888–1895. https://doi.org/10.1152/jn.01002.2009

Cressman, E.K., Henriques, D.Y.P., 2009. Sensory Recalibration of Hand Position Following Visuomotor Adaptation. J. Neurophysiol. 102, 3505–3518. https://doi.org/10.1152/jn.00514.2009

Deshpande, N., Connelly, D.M., Culham, E.G., Costigan, P.A., 2003. Reliability and validity of ankle proprioceptive measures. Arch. Phys. Med. Rehabil. 84, 883–889. https://doi.org/10.1016/s0003-9993(03)00016-9

Dietz, V., 2002. Proprioception and locomotor disorders. Nat. Rev. Neurosci. 3, 781–790. https://doi.org/10.1038/nrn939

Elangovan, N., Tuite, P.J., Konczak, J., 2018. Somatosensory Training Improves Proprioception and Untrained Motor Function in Parkinson's Disease. Front. Neurol. 9.

Emerson, P.L., 1986. Observations on maximum-likelihood and Bayesian methods of forced-choice sequential threshold estimation. Percept. Psychophys. 39, 151–153. https://doi.org/10.3758/BF03211498

Fuentes, C.T., Bastian, A.J., 2010. Where is your arm? Variations in proprioception across space and tasks. J. Neurophysiol. 103, 164–171. https://doi.org/10.1152/jn.00494.2009

652 Gandevia, S.C., 1985. Illusory movements produced by electrical stimulation of low-threshold
653 muscle afferents from the hand. Brain 108, 965–981.
654 https://doi.org/10.1093/brain/108.4.965
655 Giavarina, D., 2015. Understanding Bland Altman analysis. Biochem. Medica 25, 141–151.
656 https://doi.org/10.11613/BM.2015.015
657 Gorst, T., Freeman, J., Yarrow, K., Marsden, J., 2020. Assessing lower limb position sense in
658 stroke using the gradient discrimination test (GradDT™) and step-height discrimination
659 test (StepDT™): a reliability and validity study. Disabil. Rehabil. 42, 2215–2223.
660 https://doi.org/10.1080/09638288.2018.1554008
661 Han, J., Waddington, G., Adams, R., Anson, J., Liu, Y., 2016. Assessing proprioception: A
662 critical review of methods. J. Sport Health Sci. 5, 80–90.
663 https://doi.org/10.1016/j.jshs.2014.10.004
664 Harris, C.S., 1963. Adaptation to Displaced Vision: Visual, Motor, or Proprioceptive Change?
665 Science 140, 812–813.
666 Henriques, D.Y.P., Cressman, E.K., 2012. Visuomotor adaptation and proprioceptive
667 recalibration. J. Mot. Behav. 44, 435–444.
668 https://doi.org/10.1080/00222895.2012.659232
669 Hiebert, G.W., Whelan, P.J., Prochazka, A., Pearson, K.G., 1996. Contribution of hind limb
670 flexor muscle afferents to the timing of phase transitions in the cat step cycle. J.
671 Neurophysiol. 75, 1126–1137. https://doi.org/10.1152/jn.1996.75.3.1126
672 Hillier, S., Immink, M., Thewlis, D., 2015. Assessing Proprioception: A Systematic Review of
673 Possibilities. Neurorehabil. Neural Repair 29, 933–949.
674 https://doi.org/10.1177/1545968315573055
675 Horváth, Á., Ferentzi, E., Schwartz, K., Jacobs, N., Meyns, P., Köteles, F., 2022. The
676 measurement of proprioceptive accuracy: A systematic literature review. J. Sport Health
677 Sci. https://doi.org/10.1016/j.jshs.2022.04.001
678 Ingram, L.A., Butler, A.A., Gandevia, S.C., Walsh, L.D., 2019. Proprioceptive measurements of
679 perceived hand position using pointing and verbal localisation tasks. PLOS ONE 14,
680 e0210911. https://doi.org/10.1371/journal.pone.0210911
681 Jardine, D.L., Wieling, W., Brignole, M., Lenders, J.W.M., Sutton, R., Stewart, J., 2018.
682 Pathophysiology of the vasovagal response. Heart Rhythm 15, 921–929.
683 https://doi.org/10.1016/j.hrthm.2017.12.013
684 Jones, S.A.H., Cressman, E.K., Henriques, D.Y.P., 2010. Proprioceptive localization of the left
685 and right hands. Exp. Brain Res. 204, 373–383. https://doi.org/10.1007/s00221-009-
686 2079-8
687 Juul-Kristensen, B., Lund, H., Hansen, K., Christensen, H., Danneskiold-Samsøe, B., Bliddal,
688 H., 2008. Test-retest reliability of joint position and kinesthetic sense in the elbow of
689 healthy subjects. Physiother. Theory Pract. 24, 65–72.
690 https://doi.org/10.1080/09593980701378173
691 Kingdom, F.A.A., Prins, N., 2016. Psychophysics: A Practical Introduction. Academic Press.
692 King-smith, P.E., Rose, D., 1997. Principles of an Adaptive Method for Measuring the Slope of
693 the Psychometric Function. Vision Res. 37, 1595–1604. https://doi.org/10.1016/S0042-
694 6989(96)00310-0
695 Kontsevich, L.L., Tyler, C.W., 1999. Bayesian adaptive estimation of psychometric slope and
696 threshold. Vision Res. 39, 2729–2737. https://doi.org/10.1016/S0042-6989(98)00285-5
697 Kottner, J., Audigé, L., Brorson, S., Donner, A., Gajewski, B.J., Hróbjartsson, A., Roberts, C.,
698 Shoukri, M., Streiner, D.L., 2011. Guidelines for Reporting Reliability and Agreement
699 Studies (GRRAS) were proposed. J. Clin. Epidemiol. 64, 96–106.
700 https://doi.org/10.1016/j.jclinepi.2010.03.002

Kriellaars, D.J., Brownstone, R.M., Noga, B.R., Jordan, L.M., 1994. Mechanical entrainment of fictive locomotion in the decerebrate cat. J. Neurophysiol. 71, 2074–2086. https://doi.org/10.1152/jn.1994.71.6.2074

Kruschke, J., 2014. Doing Bayesian Data Analysis: A Tutorial with R, JAGS, and Stan. Academic Press.

Kruschke, J.K., 2013. Bayesian estimation supersedes the t test. J. Exp. Psychol. Gen. 142, 573–603. https://doi.org/10.1037/a0029146

Kruschke, J.K., Liddell, T.M., 2018. The Bayesian New Statistics: Hypothesis testing, estimation, meta-analysis, and power analysis from a Bayesian perspective. Psychon. Bull. Rev. 25, 178–206. https://doi.org/10.3758/s13423-016-1221-4

Lam, T., Pearson, K.G., 2002. The Role of Proprioceptive Feedback in the Regulation and Adaptation of Locomotor Activity, in: Gandevia, S.C., Proske, U., Stuart, D.G. (Eds.), Sensorimotor Control of Movement and Posture, Advances in Experimental Medicine and Biology. Springer US, Boston, MA, pp. 343–355. https://doi.org/10.1007/978-1-4615-0713-0_40

Leek, M.R., 2001. Adaptive procedures in psychophysical research. Percept. Psychophys. 63, 1279–1292. https://doi.org/10.3758/BF03194543

Livesey, E.J., Livesey, D.J., 2016. Validation of a Bayesian Adaptive Estimation Technique in the Stop-Signal Task. PLOS ONE 11, e0165525. https://doi.org/10.1371/journal.pone.0165525

Lord, S.R., Clark, R.D., Webster, I.W., 1991. Physiological Factors Associated with Falls in an Elderly Population. J. Am. Geriatr. Soc. 39, 1194–1200. https://doi.org/10.1111/j.1532-5415.1991.tb03574.x

Lord, S.R., Ward, J.A., 1994. Age-associated differences in sensori-motor function and balance in community dwelling women. Age Ageing 23, 452–460.

Mattar, A.A.G., Darainy, M., Ostry, D.J., 2013. Motor learning and its sensory effects: time course of perceptual change and its presence with gradual introduction of load. J. Neurophysiol. 109, 782–791. https://doi.org/10.1152/jn.00734.2011

McElreath, R., 2016. Statistical Rethinking: A Bayesian Course with Examples in R and Stan. CRC Press.

McGraw, K.O., Wong, S.P., 1996. Forming inferences about some intraclass correlation coefficients. Psychol. Methods 1, 30–46. https://doi.org/10.1037/1082-989X.1.1.30

Nicholson, L., Adams, R., Maher, C., 1997. Reliability of a discrimination measure for judgements of non-biological stiffness. Man. Ther. 2, 150–156. https://doi.org/10.1054/math.1997.0295

Ostry, D.J., Darainy, M., Mattar, A.A.G., Wong, J., Gribble, P.L., 2010. Somatosensory Plasticity and Motor Learning. J. Neurosci. 30, 5384–5393. https://doi.org/10.1523/JNEUROSCI.4571-09.2010

Pearson, K.G., 2004. Generating the walking gait: role of sensory feedback. Prog Brain Res 143, 123–9. https://doi.org/10.1016/S0079-6123(03)43012-4

Pearson, K.G., 2000. Neural Adaptation in the Generation of Rhythmic Behavior. Annu. Rev. Physiol. 62, 723–753. https://doi.org/10.1146/annurev.physiol.62.1.723

Portney, L.G., Watkins, M.P., 2009. Foundations of clinical research: applications to practice. Pearson/Prentice Hall Upper Saddle River, NJ.

Prokop, T., Berger, W., Zijlstra, W., Dietz, V., 1995. Adaptational and learning processes during human split-belt locomotion: interaction between central mechanisms and afferent input. Exp. Brain Res. 106, 449–456. https://doi.org/10.1007/BF00231067

Proske, U., Gandevia, S.C., 2012. The Proprioceptive Senses: Their Roles in Signaling Body Shape, Body Position and Movement, and Muscle Force. Physiol. Rev. 92, 1651–1697. https://doi.org/10.1152/physrev.00048.2011

751 Rahlf, A.L., Petersen, E., Rehwinkel, D., Zech, A., Hamacher, D., 2019. Validity and Reliability
752 of an Inertial Sensor-Based Knee Proprioception Test in Younger vs. Older Adults.
753 Front. Sports Act. Living 1, 27. https://doi.org/10.3389/fspor.2019.00027
754 Reisman, D.S., Block, H.J., Bastian, A.J., 2005. Interlimb coordination during locomotion: what
755 can be adapted and stored? J. Neurophysiol. 94, 2403–2415.
756 https://doi.org/10.1152/jn.00089.2005
757 Relph, N., Herrington, L., Tyson, S., 2014. The effects of ACL injury on knee proprioception: a
758 meta-analysis. Physiotherapy 100, 187–195.
759 https://doi.org/10.1016/j.physio.2013.11.002
760 Ribeiro, F., Oliveira, J., 2007. Aging effects on joint proprioception: the role of physical activity in
761 proprioception preservation. Eur. Rev. Aging Phys. Act. 4, 71–76.
762 https://doi.org/10.1007/s11556-007-0026-x
763 Rinderknecht, M.D., Lambercy, O., Raible, V., Büsching, I., Sehle, A., Liepert, J., Gassert, R.,
764 2018. Reliability, validity, and clinical feasibility of a rapid and objective assessment of
765 post-stroke deficits in hand proprioception. J. NeuroEngineering Rehabil. 15, 47.
766 https://doi.org/10.1186/s12984-018-0387-6
767 Roden-Reynolds, D.C., Walker, M.H., Wasserman, C.R., Dean, J.C., 2015. Hip proprioceptive
768 feedback influences the control of mediolateral stability during human walking. J.
769 Neurophysiol. 114, 2220–2229. https://doi.org/10.1152/jn.00551.2015
770 Ruttle, J.E., 't Hart, B.M., Henriques, D.Y.P., 2021. Implicit motor learning within three trials. Sci.
771 Rep. 11, 1627. https://doi.org/10.1038/s41598-021-81031-y
772 Salvatier, J., Wiecki, T.V., Fonnesbeck, C., 2016. Probabilistic programming in Python using
773 PyMC3. PeerJ Comput. Sci. 2, e55. https://doi.org/10.7717/peerj-cs.55
774 Santuz, A., Laflamme, O.D., Akay, T., 2022. The brain integrates proprioceptive information to
775 ensure robust locomotion. J. Physiol. https://doi.org/10.1113/JP283181
776 Schilling, T., Ohlendorf, A., Leube, A., Wahl, S., 2017. TuebingenCSTest – a useful method to
777 assess the contrast sensitivity function. Biomed. Opt. Express 8, 1477–1487.
778 https://doi.org/10.1364/BOE.8.001477
779 Shannon, C.E., 1948. A mathematical theory of communication. Bell Syst. Tech. J. 27, 379–
780 423. https://doi.org/10.1002/j.1538-7305.1948.tb01338.x
781 Sigmundsson, H., Whiting, H.T.A., Loftesnes, J.M., 2000. Development of proprioceptive
782 sensitivity. Exp. Brain Res. 135, 348–352. https://doi.org/10.1007/s002210000531
783 Silva, G.M., Souto, J.J., Fernandes, T.P., Bonifacio, T.A., Almeida, N.L., Gomes, G.H.,
784 Felisberti, F.M., Santos, N.A., 2020. Impairments of facial detection in tobacco use
785 disorder: baseline data and impact of smoking duration. Braz. J. Psychiatry 43, 376–384.
786 https://doi.org/10.1590/1516-4446-2020-1107
787 Simani, M.C., McGuire, L.M.M., Sabes, P.N., 2007. Visual-Shift Adaptation Is Composed of
788 Separable Sensory and Task-Dependent Effects. J. Neurophysiol. 98, 2827–2841.
789 https://doi.org/10.1152/jn.00290.2007
790 Soechting, J.F., 1982. Does position sense at the elbow reflect a sense of elbow joint angle or
791 one of limb orientation? Brain Res. 248, 392–395. https://doi.org/10.1016/0006-
792 8993(82)90601-1
793 Sombric, C., Gonzalez-Rubio, M., Torres-Oviedo, G., 2019. Split-Belt walking induces changes
794 in active, but not passive, perception of step length. Sci. Rep. 9, 16442.
795 https://doi.org/10.1038/s41598-019-52860-9
796 Stillman, B.C., McMeeken, J.M., 2001. The role of weightbearing in the clinical assessment of
797 knee joint position sense. Aust. J. Physiother. 47, 247–253.
798 https://doi.org/10.1016/S0004-9514(14)60272-5
799 Strong, A., Srinivasan, D., Häger, C.K., 2021. Development of supine and standing knee joint
800 position sense tests. Phys. Ther. Sport Off. J. Assoc. Chart. Physiother. Sports Med. 49,
801 112–121. https://doi.org/10.1016/j.ptsp.2021.02.010

802 Talbot, L.A., Musiol, R.J., Witham, E.K., Metter, E.J., 2005. Falls in young, middle-aged and
803 older community dwelling adults: perceived cause, environmental factors and injury.
804 BMC Public Health 5, 86. https://doi.org/10.1186/1471-2458-5-86
805 Tsay, J.S., Kim, H., Haith, A.M., Ivry, R.B., 2022. Understanding implicit sensorimotor
806 adaptation as a process of proprioceptive re-alignment. eLife 11, e76639.
807 https://doi.org/10.7554/eLife.76639
808 Tsay, J.S., Kim, H.E., Parvin, D.E., Stover, A.R., Ivry, R.B., 2021. Individual differences in
809 proprioception predict the extent of implicit sensorimotor adaptation. J. Neurophysiol.
810 125, 1307–1321. https://doi.org/10.1152/jn.00585.2020
811 Turpin, A., Jankovic, D., McKendrick, A., 2010. Identifying steep psychometric function slope
812 quickly in clinical applications. Vision Res., Vision Research Reviews 50, 2476–2485.
813 https://doi.org/10.1016/j.visres.2010.08.032
814 van Beers, R.J., Sittig, A.C., Denier van der Gon, J.J., 1998. The precision of proprioceptive
815 position sense. Exp. Brain Res. 122, 367–377. https://doi.org/10.1007/s002210050525
816 van Beers, R.J., Sittig, A.C., van der Gon Denier, J.J., 1996. How humans combine
817 simultaneous proprioceptive and visual position information. Exp. Brain Res. 111, 253–
818 261. https://doi.org/10.1007/BF00227302
819 van Beers, R.J., Wolpert, D.M., Haggard, P., 2002. When feeling Is more important than seeing
820 in sensorimotor adaptation. Curr. Biol. 12, 834–837. https://doi.org/10.1016/S0960-
821 9822(02)00836-9
822 Vazquez, A., Statton, M.A., Busgang, S.A., Bastian, A.J., 2015. Split-belt walking adaptation
823 recalibrates sensorimotor estimates of leg speed but not position or force. J.
824 Neurophysiol. https://doi.org/10.1152/jn.00302.2015
825 Vindras, P., Desmurget, M., Prablanc, C., Viviani, P., 1998. Pointing Errors Reflect Biases in the
826 Perception of the InitialHand Position. J. Neurophysiol. 79, 3290–3294.
827 https://doi.org/10.1152/jn.1998.79.6.3290
828 Waddington, G., Adams, R., 1999. Discrimination of active plantarflexion and inversion
829 movements after ankle injury. Aust. J. Physiother. 45, 7–13.
830 https://doi.org/10.1016/s0004-9514(14)60335-4
831 Wasserstein, R.L., Lazar, N.A., 2016. The ASA Statement on *p* -Values: Context, Process, and
832 Purpose. Am. Stat. 70, 129–133. https://doi.org/10.1080/00031305.2016.1154108
833 Watson, A.B., Fitzhugh, A., 1990. The method of constant stimuli is inefficient. Percept.
834 Psychophys. 47, 87–91. https://doi.org/10.3758/BF03208169
835 Whelan, P.J., Hiebert, G.W., Pearson, K.G., 1995. Stimulation of the group I extensor afferents
836 prolongs the stance phase in walking cats. Exp. Brain Res. 103, 20–30.
837 https://doi.org/10.1007/BF00241961
838 Wolpert, D.M., Ghahramani, Z., Jordan, M.I., 1995. An internal model for sensorimotor
839 integration. Science 269, 1880–1882. https://doi.org/10.1126/science.7569931
840
841

Figures and Tables

Figure 1:

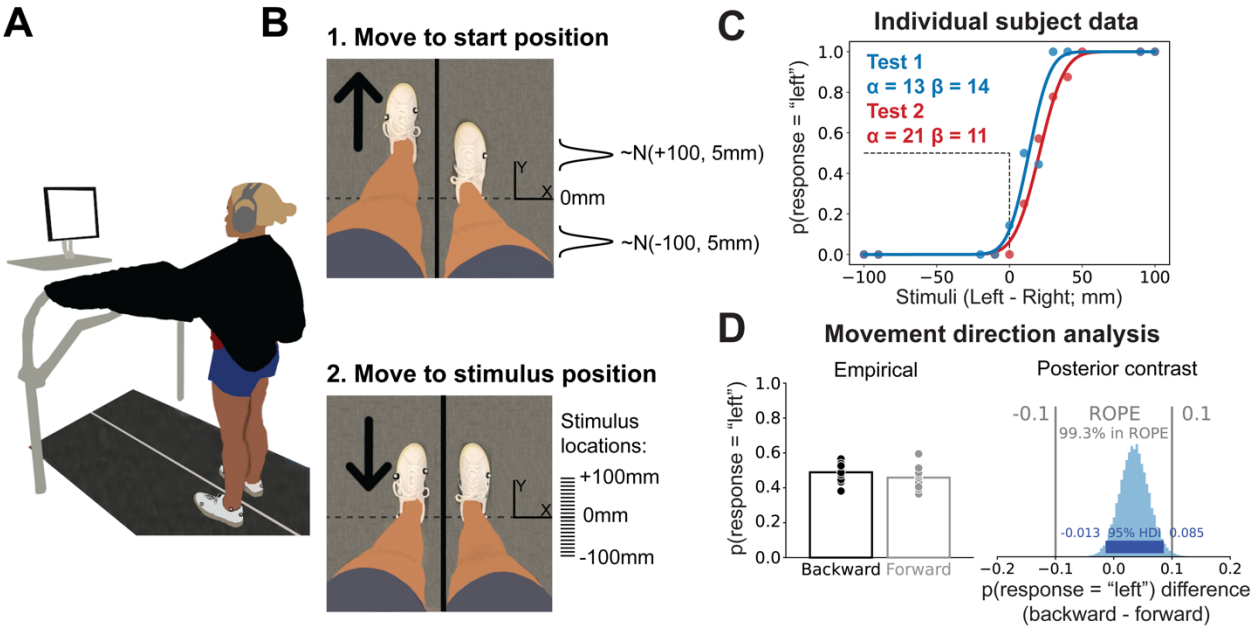

Figure 2:

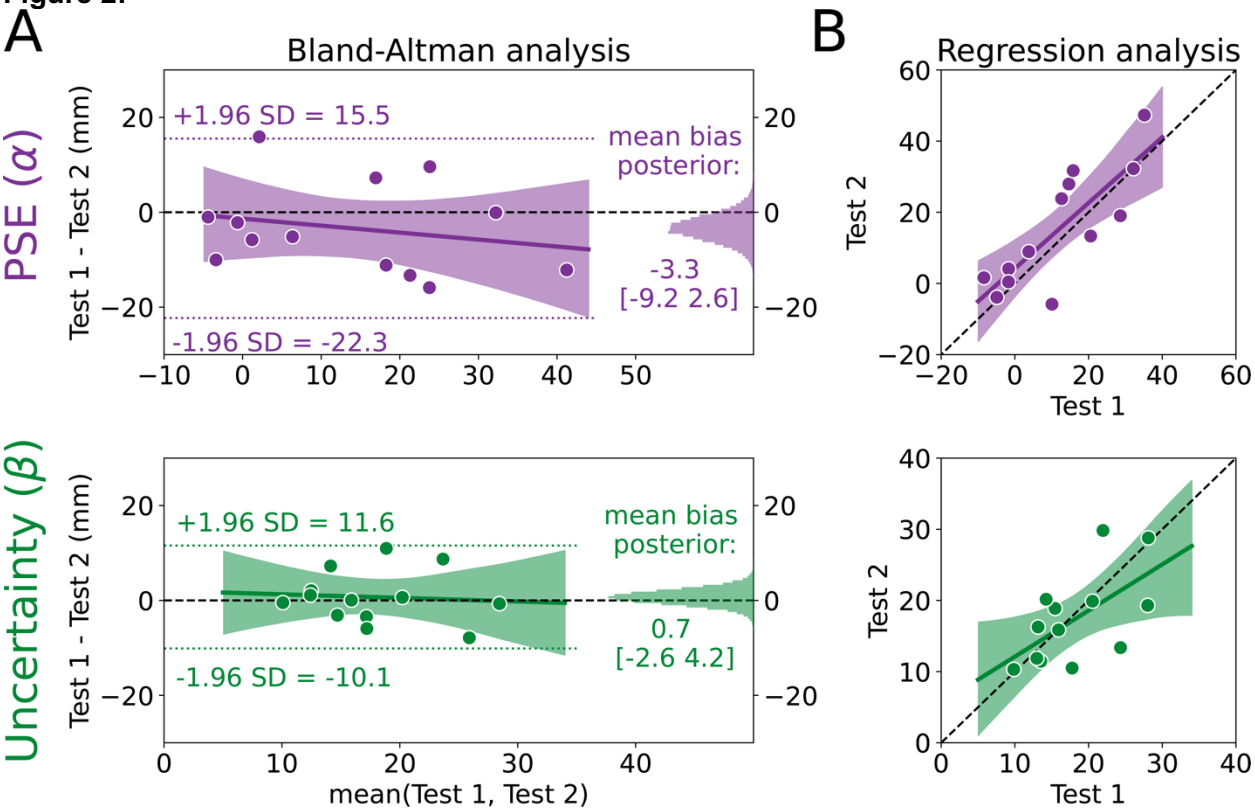

853 **Table 1: Agreement comparison after 50 and 75 trials**

	Limits of agreement (mm)	Bland Altman Mean Bias (mm; % in ROPE)	Bland Altman Bias Regression (mm; % in ROPE)	Test 1 vs Test 2 Regression	$ICC_{2,1}$ [95% CI]
PSE (α)					
50 trials	-22.3 to 15.7	-3.2 [-9.2 2.6] (73.5%)	Slope = -0.17 [-0.61 0.29] (26.2%) Intercept = -1.1 [-9.3 7.1] (77.0%)	Slope= 0.91 [0.45 1.40] Intercept = 4.1 [-3.9 12.0]	0.78 [0.43, 0.92]
75 trials	-22.3 to 15.5	-3.3 [-9.0 2.8] (72.4%)	Slope = -0.15 [-0.56 0.28] (29.6%) Intercept = -1.3 [-9.5 6.9] (76.0%)	Slope= 0.92 [0.49 1.38] Intercept = 4.2 [-3.7 12.4]	0.80 [0.48, 0.93]
Uncertainty (β)					
50 trials	-9.3 to 10.2	0.5 [-2.7 3.5] (99.5%)	Slope = 0.03 [-0.65 0.69] (24.3%) Intercept = 0.0 [-12.5 12.2] (60.0%)	Slope= 0.57 [0.03 1.09] Intercept = 7.4 [-2.8 17.4]	0.58 [0.05, 0.85]
75 trials	-10.1 to 11.6	0.7 [-2.8 4.1] (98.8%)	Slope = -0.08 [-0.69 0.58] (24.5%) Intercept = 2.0 [-9.8 13.8] (58.4%)	Slope= 0.65 [0.09 1.19] Intercept = 5.6 [-5.6 15.8]	0.61 [0.05, 0.86]

854

Figure Captions

Figure 3. Task setup, representative data, and movement direction analysis. (A) AFC task setup. Participants stood on the split-belt treadmill with visual feedback of their legs occluded by a black drape and auditory feedback occluded by noise cancelling headphones. The screen prompted participants to verbally respond to the question “Do you feel like your right or left foot is more forward?” when the test foot stopped at the stimulus location. **(B)** Trial sequence. 1) The test foot was moved to a start position either in front of or behind the stimulus position. Start positions were sampled from one of two normal distributions, depending on the movement direction assigned for that specific trial. 2) The test foot was moved to one of 21 possible stimulus positions between -100 and +100 mm. Tick marks (drawn to scale) represent each possible stimulus location. **(C)** Individual participant data. We reconstructed the psychometric functions from the PSE (α) and uncertainty (β) estimates for Test 1 (blue) and Test 2 (red). The dashed black lines, provided as a reference, represent a PSE of 0 mm. The individual dots represent the participant’s response data for each test. **(D)** Movement direction analysis. We measured the mean empirical probability of responding left when the movement direction to the stimulus position was forward (gray) vs backward (black). Dots represent individuals. We also used a Bayesian logistic regression model to analyze the unique impact of each movement direction on participant responses by calculating the difference between the posterior estimates of the movement direction coefficients (one for forward movement, one for backwards) of every participant, yielding a posterior contrast distribution (histogram) which we compared to a region of practical equivalence (ROPE). We note that 99.3% of the posterior distribution is within the ROPE, confirming that responses were not biased by movement direction to the stimulus position.

Figure 4: Point of subjective equality (PSE) and uncertainty estimates have good agreement. (A) Bland-Altman plot for the PSE (α; top) and uncertainty (β; bottom) estimates. The mean of Test 1 and Test 2 for each individual is plotted on the x-axis and the difference between the two tests is plotted on the y-axis. Thus, each dot represents one individual. The limits of agreement are plotted as the dotted lines, and the posterior distributions for the mean biases are plotted on the right sides as histograms. The most probable regression line is the solid line with the shading representing the 95% high density interval (HDI), with the black dashed line at 0 as a reference **(B)** Regression model for PSE and uncertainty. Estimates for Test 2 are plotted against estimates for Test 1 for each individual (dots) with the unity line (black dashed line) provided as a reference for perfect agreement. The most probable regression line is the solid line with the shading representing the 95% HDI.